

FEM-based Simulation of Stress Distribution in U71Mn Heavy Rail during Quenching

**Siqiang Xu, Jianyi Kong, Gongfa Li, Jintang Yang, Hegen Xiong
and Guozhang Jiang**

College of Machinery and Automation,
Box 242, Wuhan University of Science and Technology, Wuhan, 430081, China
Tel.: +86-15927505887
E-mail: xusiqiang@yahoo.com.cn

Received: 11 September 2012 /Accepted: 11 October 2012 /Published: 20 November 2012

Abstract: Quenching is one of the crucial heat treatment processes for manufacture of components with desired mechanical properties. Success or failure of a quenching process is identified by arranging an appropriate technique. In this work, the quenching process of U71Mn heavy rails with different parameters including heating time, cooling time and air pressure was investigated. The stress distribution of the rail-ends during the quenching process was simulated by the finite element method. The equivalent heat capacity method which handles the effect of latent heat, that is, heat energy that the heavy rail releases during a phase change, on the temperature field, was utilized in the simulation computation, in addition to the equivalent linear expansion coefficient method which deals with the transformation stress introduced from a phase change. In the meantime, the effect of material's non-linear parameters on the temperature field was taken into consideration. The research result indicates that the air-blast quenching introduces minor residual stress and avoids heavy rail's deformation and cracking. *Copyright © 2012 IFSA.*

Keywords: Heavy rail, Quenching process, Finite element method, Stress distribution, Residual stress.

1. Introduction

Quenching, as one of main approaches, can improve material mechanical properties such as toughness and wear resistance. It turns out that heavy rails, whose ends are quenched, improve not only their strength and lifetime but also sharply reliable service properties. Distortion, cracking, achievement of desired distribution of microstructure and residual stresses are considered to be the most important

problems during quenching of steels, which render the prediction and control of the as-quenched state of the component into a vital process in order to achieve production goals.

A precise knowledge of the magnitudes of residual stresses that exist in safety critical engineering components is necessary [1]. Success or failure of heat treatment not only affects manufacturing costs but also determines product quality and reliability. Heat treatment must therefore be taken into account during development and design, and it has to be controlled in the manufacturing process. For this reason, modeling of heat treatment processes has a great importance to engineers and scientists. In the last three decades, the modeling of residual stress and distortion induced by quenching has received considerable attention and the finite element method (FEM) is utilized more and more often to compute temperature and stress fields during quenching. Denis [2] investigated effects of stress on the phase transformation kinetics and transformation plasticity using a coupled model of a cylinder. Inoue and Arimoto [3] developed a CAE system, based on Metallo-Thermo-Mechanics theory, for heat treatment simulation. Heming [4] used finite element analysis to determine the residual stress field in a steel cylinder. Sen S [5] also used finite element analysis to predict the residual and thermal stresses which occurred during water quenching of solid cylindrical rods and ring cross-sectioned steel tubes. Caner Simsir [6] developed a 3D FEM based model, which is integrated into commercial FEA software Msc. Marc via user subroutines, to predict temperature history, evolution of microstructure and internal stresses during quenching, and investigate of the effect of asymmetric geometry on residual stress distribution.

In this paper, the stress distribution was simulated during the rail-end quenching and its causes were investigated. In addition, the numerical simulation was carried out in order to improve the quenching process to diminish the internal stress during quenching.

2. Causes of Thermal Stress during Rail's Quenching

Cooling during quenching can be uneven, which translates into large thermal gradients that cause residual stresses. In practical manufacturing, the quenching process was that rail-ends were cooled by means of air-blast cooling in conjunction with free cooling after heating and holding in order to enhance production efficiency, as shown in Fig. 1. Rail-end surface temperature descended sharply during the wind-cooling process, meantime, the workpiece internal layer was contracted and deformed as it was cooled through heat conduction (The inner layer deformed easily owing to high temperature), and then it constructed a compressive stress against the external layer. The stress state in the external layer was transformed from the initial tensile stress during cooling contraction into the final compressive stress after cooling and deposited in the form of residual stress after quenching.

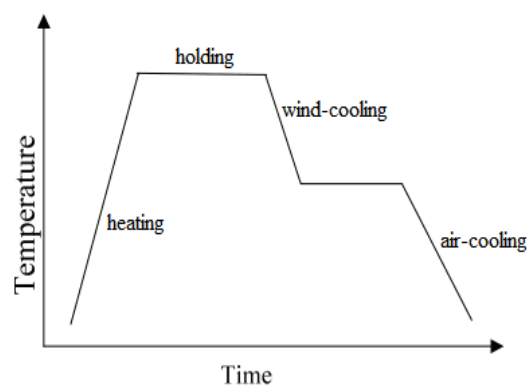


Fig. 1. The quenching process of heavy rail.

The change law of the residual stress during the entire wind-cooling of rail-ends was: during the early stages of cooling, the surface was placed in tension but the center was placed in compression; during the latter stages of cooling, the surface was compressed while the center was tensed. The final residual stress state at the end of cooling was that the residual stress is compressive close to the surface whereas the residual stress is tensile close to the center. As it showed, variety for the thermal stress introduced during the rail-end quenching was complex and instantaneous. The change law as a function of time couldn't be illustrated precisely by formulas or experience. However, not only the thermal stress distribution at a certain time during the quenching process could be simulated, but the stress concentration and magnitude also were attained directly by the finite element method.

3. Stress Distribution during Quenching

3.1. Technique of Rail-end Quenching

The chemical composition of materials used for U71Mn heavy rails was shown in Table 1. The heavy rail's heat-treatment technique involved as follow: firstly the section 200 mm apart from the rail-end was heated to 910 °C for 40 s in the electromagnetic field, secondly held for 5 s, thirdly cooled for 25 s by intensive convection of cold air and at last air cooled to ambient temperature. The wind-cooling apparatus was shown in Fig. 2.

Table 1. Chemical composition of materials used for U71Mn heavy rails (wt%).

Brand name	Chemical composition (%)				
	C	Si	Mn	P	S
U71Mn	0.365~0.77	0.15~0.35	1.10~1.50	<0.040	<0.040

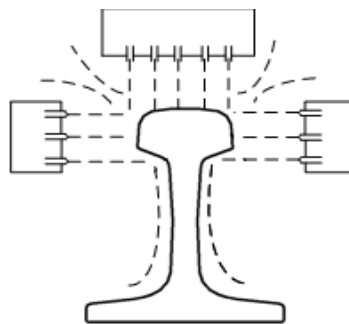


Fig. 2. The sketch of the wind-cooling apparatus.

3.2. Establish Model and Solution

The heavy-rail's three-dimensional model, which was carried out according to the size regulated by YB(T) 68-1987 standards for the heavy rail of 60 kg/m using a three-dimensional software, was imported into the finite element analysis software to be swept with the element SOLID5 to obtain the FEM shown in Fig. 4, as presented in Fig. 3.

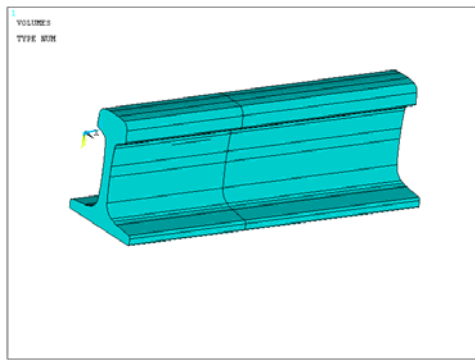


Fig. 3. Model of heavy rail.

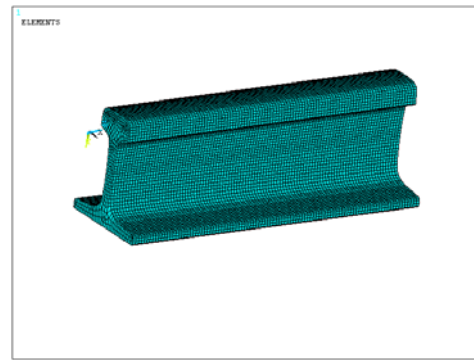


Fig. 4. FEM of heavy rail.

The direction of magnetic induction lines was guaranteed parallel to the rail-ends boundary by setting boundary conditions for the electromagnetic field; distribution of induction current of the magnetic field was calculated by loading in coils alternating current, whose magnitude, frequency and time were $1.12e6$ (A/m²), 1000 Hz and 40 s, respectively. Then the magnetic field was loaded into the temperature field as initial conditions by the sequential coupled approach, meanwhile, initial temperature was set to 25 °C and temperature distribution was attained at this load. At last the temperature histories were loaded on the FEM to solve as initial conditions for stresses. Stress distribution in the rail-end was obtained namely.

Referring to the Materials Handbook, the rail-end density was 7920 kg/m³, besides, the rest of main physical properties were shown in Table 2. Heavy-rail's thermal physical parameters, such as relative permeability, specific heat, resistivity and thermal conductivity, varied with temperature from the Table. Moreover, convective heat-transfer coefficient for the rail-end was severely non-linear during wind-cooling, as shown in Fig. 5. They were applied to load in tabular method in application.

Table 2. Parameters of materials for rail-ends.

T[°C]	25	100	200	300	400	500	600	700	800	900	1000	1100
Relative Permeability	200	194.5	187.6	181	169.8	157.3	140.8	100.4	1	1	1	1
Specific heat J/[g°C]	472	480	498	524	560	615	700	1000	806	637	602	580
Resistivity [Ω]	1.84e-007	2.54e-007	3.39e-007	4.35e-007	5.41e-007	6.56e-007	7.9e-007	9.49e-007	1.08e-006	1.16e-006	1.20e-006	1.23e-006
Enthalpy[J/m ³]	9.16e+007	3.56e+008	7.53e+008	1.16e+009	1.63e+009	2.12e+009	2.65e+009	3.19e+009	3.72e+009	4.22e+009	4.52e+009	5.14e+009
Thermal conductivity [W/(m·°C)]	93.23	87.68	83.53	80.44	78.13	76.02	74.16	71.98	68.66	66.49	65.92	64.02

3.3. Analysis of Factors Influencing Distribution for Thermal Stress Field in the Heavy-rail

Factors influencing distribution of thermal stress field in the heavy-rail were chiefly heating, holding time and pressure of compressed air during cooling through researching and discovering the heavy-rail's quenching process.

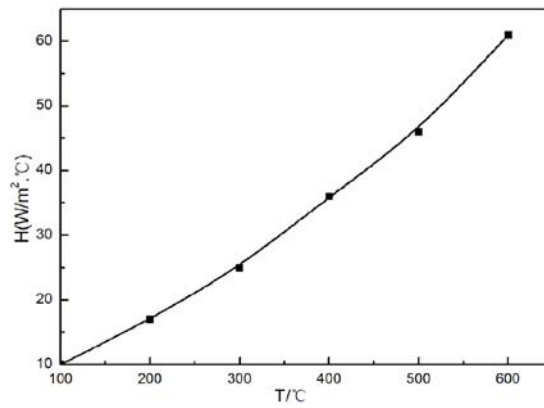
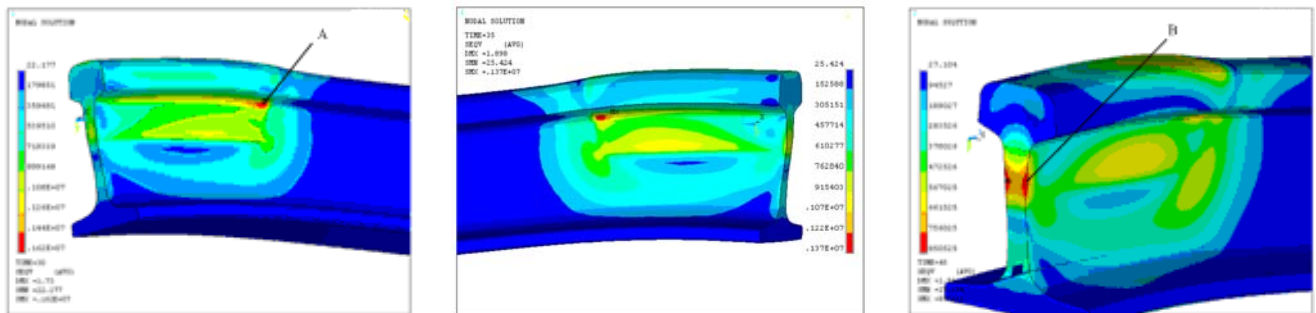


Fig. 5. Heat transfer coefficient of heavy ends during wind cooling.

(a) Stress distributions in the rail-end heated for 30 s, heated for 30 s and then held for 5 s, heated for 30 s, then held for 5 s and at last cooled for 25 s by compressed air were shown in Fig. 6(a), Fig. 6(b) and Fig. 6(c), respectively; stress distributions in the rail-end heated for 35 s, heated for 35 s and then held for 10 s, heated for 35 s, then held for 10 s and at last cooled for 25 s by compressed air were shown in Fig. 7(a), Fig. 7(b) and Fig. 7(c), respectively.

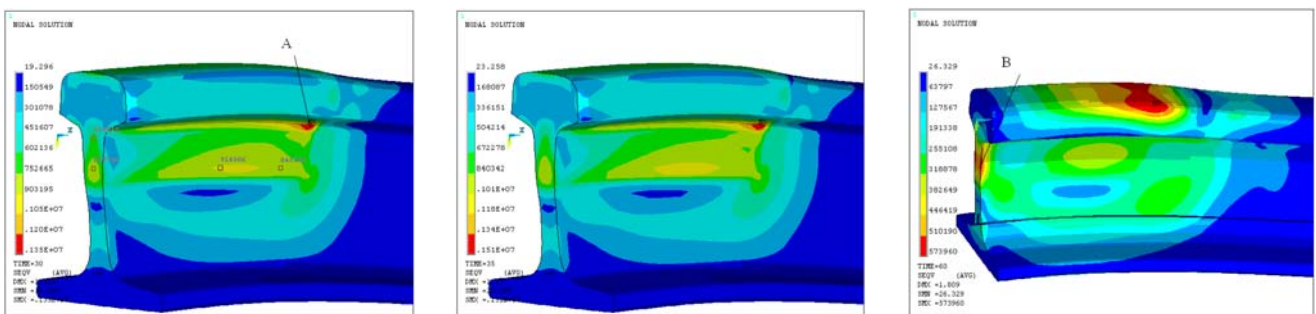


(a) t=30 s

(b) t=35 s

(c) t=60 s

Fig. 6. Stress distribution of heavy rail at different time when p=0.4 MPa (heated for 30 s).



(a) t=35 s

(b) t=45 s

(c) t=70 s

Fig. 7. Stress distribution contours of heavy rail at different time when p=0.4 MPa (heated for 35 s).

It was found through analyzing stress distribution contours that locations of maximum stresses during heating in two heating manners were at A zone which was shown in Fig. 6(a) and Fig. 7(a), respectively.

And maximum stress values were 1.62 MPa and 1.35 MPa, respectively. This occurred because A zone was located at transition region between the heated region and unheated region. The heated region swelled and its volume expanded owing to temperature rising while expansion was not large and volume change was less in unheated region as a consequence of minor heat. As a result, A zone was compressed and subjected to compressive stress since volume change in two regions was nonuniform.

In the meantime, it was also found that locations of maximum stresses at the end of wind cooling were at B zone which was shown in Fig. 6(c) and Fig. 7(c), respectively. And maximum stress values were 0.8 MPa and 0.5 MPa, respectively. The main reason was that radiating area at the position of the B zone was less due to the cross section vertical to the rail-end's longitudinal section during wind cooling. The thermal stress at the location was the largest.

In addition, it was found through comparing stress values in B region of Fig. 6(c) with that of Fig. 7(c) that the residual stress in Fig. 7(c) was less since more time for heating and holding helped to transfer heat, meanwhile, volume accommodation in the heated region was supplied with more time and higher temperature. Then the heated region was made to diminish compression on the A zone through self-deformation under the compressive stress in unheated regions.

It was discovered with numerous comparative analyses that heating time of rail-ends could not be less than 30 s but redundant heating time would decrease production efficiency for heavy-rails. Heating time could be set to 40 ± 1 s after both them were taken into consideration comprehensively.

(b) Stress field distribution in the rail-end cooled by forced air for 40 s, 50 s and 60 s at pressure of 0.4 MPa were shown as Fig. 8(a), Fig. 8(b) and Fig. 8(c), respectively; stress field distributions in the rail-end cooled by forced air for 40 s, 50 s and 60 s at pressure of 0.8 MPa were shown as Fig. 9(a), Fig. 9(b) and Fig. 9(c), respectively.

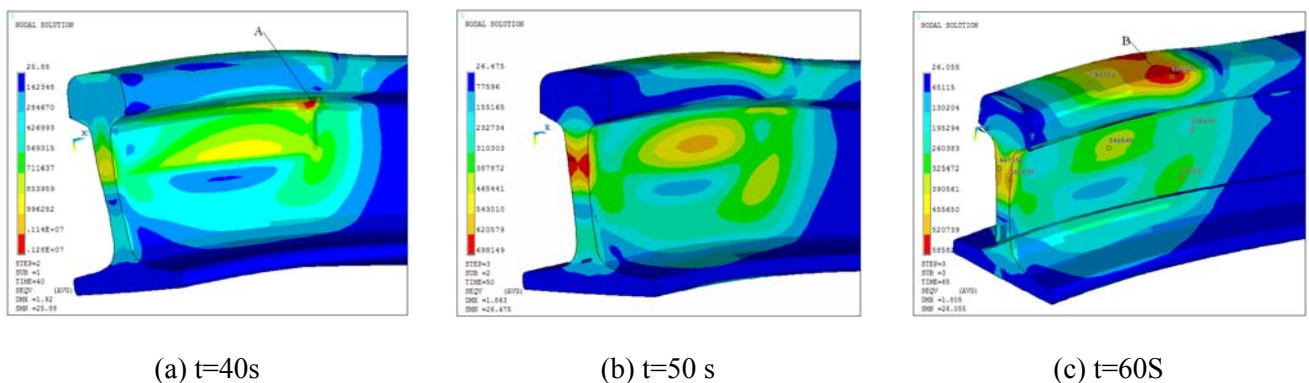


Fig. 8. Stress distribution of heavy rail at various time when $p=0.4$ MPa (heated for 30 s).

Analyses of Fig. 8 and Fig. 9 performed, it was obtained that concentration regions of stresses, whose values were 1.28 MPa uniformly, were A zone shown in Fig. 8(a) and Fig. 9(a) after 40 s during wind cooling; concentration regions of the residual stress, whose values were 0.59 MPa and 0.56 MPa, respectively, was B zone shown in Fig. 8(c) and Fig. 9(c) at the end of cooling.

Comparison between the residual stress value in Fig. 8(c) and that in Fig. 9(c) was achieved. It indicated that residual thermal stress of rail-ends was less when they were cooled by compressed air at pressure of 0.8 MPa. This was because compressed air at the pressure of 0.8 MPa possessed better the behavior for convective heat-transfer and could diminish temperature more rapidly in the heated region. As a result, it shortened time of compressing B zone and decreased thermal stress.

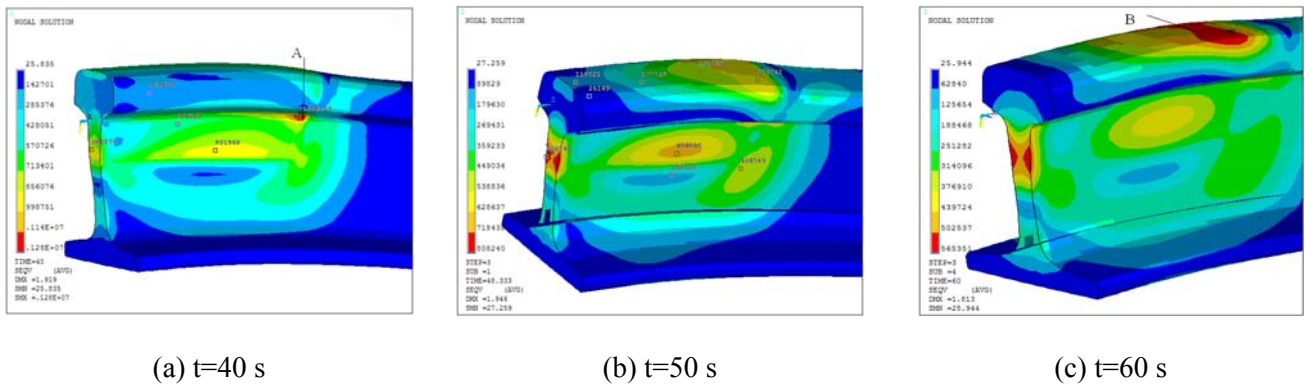


Fig. 9. Stress distribution of heavy rail at various time when $p=0.8$ MPa (heated for 30 s).

From the above analysis, pressure of compressed air was set at 0.8 MPa in practical manufacturing in order to diminish residual stress and consider cost simultaneously.

4. Analysis of Structural Stress after Rail-end Quenching

The above analysis revealed that the significant reason why thermal stress occurred during rail-end quenching was that transition region due to differences in the amount of thermal expansion and contraction between heated and unheated regions in rail-ends was compressed to introduce stress.

In addition, the rail ends during wind cooling, various structural transformations arising from differences of cooling velocity between surfaces and centers in heated regions also introduced structural stresses in heated regions. When wind cooling of the rail-end started from the temperature of 910 °C, the surface cooled rather rapidly and transformation to ferrite with the attendant volume expansion occurred there. Whereas the center volume remained stubbornly unchanged as there was austenite in the center. Structural stresses were presented that the center averting surface volume expansion was placed in tensile stress while at the same time the surface restrained by the center was placed in compressive stress; during the latter stages of cooling, surface volume stopped contracting, and the center continued cooling with volume contraction. The thermal stresses were that the center opposed by the surface was subjected to tensile stress whereas the surface, in turn, was subjected to compressive stress.

In order to reduce residual stress, heating time was extended as long as possible and larger pressure was taken, besides, time for cooling rail-ends during air cooling was as long as possible to balance the tensile and compressive stress at surfaces and centers of rail-ends taking advantages of aging. The comparison of stress histories for the surface and center nodes, which were air cooled (for 1850s) after they were cooled for 40 s by compressed air at the pressure of 0.8 MPa, was shown in Fig. 10. The fact that the longer time cooled in the air was, the less the stress difference between the rail-end surface and center was attained.

5. Conclusions

Common action between thermal and structural stress during the rail-end quenching made distribution of internal stress in the workpiece extraordinarily complex since both acted reversely and were difficult to be measured. In generally, stress and deformation in the rail-end during heat treatment were assessed indirectly through gauging final stress and deformation after heat treatment. It was of lag and apparently

had a bad effect on production for heavy-rails. In this paper, stress distribution for the rail-end during quenching was simulated successfully by the FEM. Based on considering cost, the method, that pressure of forced air was set at 0.8 MPa, then heating and holding time of the rail-end was set to 40 ± 1 s and 5 s, respectively, and at last it was cooled for 1850s in the air after it was cooled for 40 s by compressed air, of the residual stress relief was proposed. Practical productive operation in a certain steel and iron corporation indicated that these strategies were helpful to actual production of heavy rails and possessed a certain popularizing value.

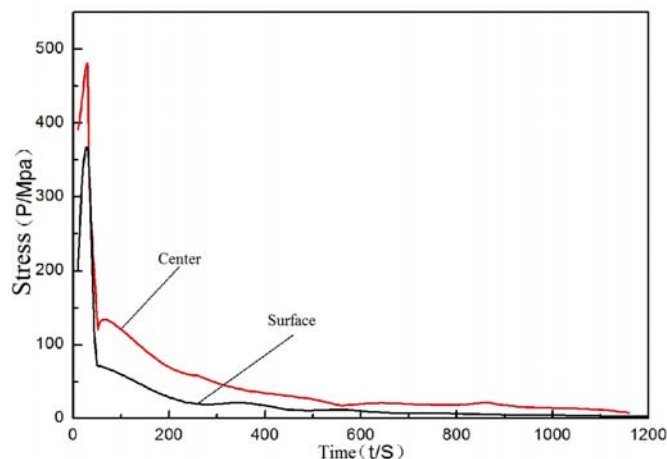


Fig. 10. Comparison of stress histories for between the surface and center node.

Acknowledgements

This research reported in the paper is supported by Research Center of Green manufacturing and Energy-Saving & Emission Reduction Technology in Wuhan University of Science and Technology. This support is greatly acknowledged.

References

- [1]. Webster GA, Role of residual stress in engineering applications, *Materials Science Forum*, Vol. 347-349, 2000, pp. 1–9.
- [2]. Denis S, Sjöström S, Simon A, Coupled temperature, stress, phase transformation calculation model numerical illustration of the internal stresses evolution during cooling of a eutectoid carbon steel cylinder, *Metall. Mater. Trans. A*, Vol. 18, 1987, pp. 1203-1212.
- [3]. Inoue T, Arimoto K, Development, implementation of CAE system “HEARTS” for heat treatment simulation based on metallo-thermo-mechanics, *J. Mater. Eng. Perform*, Vol. 6, 1997, pp. 51-60.
- [4]. Heming C, Xieqing H, Honggang W, Calculation of the residual stress of a 45 steel cylinder with a non-linear surface heat-transfer coefficient including phase transformation during quenching, *Journal of Materials Processing Technology*, Vol. 89-90, 1999, pp. 339-343.
- [5]. Sen S, Aksakal B, Ozel A, Transient and residual thermal stresses in quenched cylindrical bodies, *International Journal of Mechanical Sciences*, Vol. 42, 2000, pp. 2013-2029.
- [6]. Caner Simsir, C Hakan Gur, 3D FEM simulation of steel quenching and investigation of the effect of asymmetric geometry on residual stress distribution, *Journal of Materials Processing Technology*, Vol. 207, 2008, pp. 211-221.
- [7]. Guozhang Jiang, Jianyi Kong and Gongfa Li, Research on Temperature Distribution Model of Ladle and Its Test, *China Metallurgy*, Vol. 16, Issue 11, 2006, pp. 30-36.
- [8]. Gongfa Li, Jianyi Kong and Jintang Yang, Simulation on Temperature Field of Heavy Rail during Quenching, *Heat Treatment Technology and Equipment*, Vol. 30, Issue 1, 2009, pp. 13-15.

- [9]. Jianyi Kong, Siqiang Xu, Gongfa Li, Jintang Yang, Hegen Xiong and Guozhang Jiang: Temperature Field and Its Influencing Factors of Heavy Rail During Quenching, *Advanced Materials Research*, Vol. 15, 2010, pp. 65-69.
- [10]. Zhang Zhaohui, ANSYS Thermal Analysis Tutorials and Example Analysis, *China Railway Press*, Beijing, 2007.

2012 Copyright ©, International Frequency Sensor Association (IFSA). All rights reserved.
(<http://www.sensorsportal.com>)



**Easy and quick
sensors systems development**

**Evaluation Kit CD
EVAL UFDC-1/UFDC-1M-16**

International Frequency
Sensor Association
IFSA

OPTYS Corporation
**OPTYS
CORPORATION**

- 16 measuring modes
- Frequency range from 0.05 Hz up to 7.5 MHz (120 MHz)
- Programmable accuracy from 1 % up to 0.001 %
- RS232 (USB optional)

sales@sensorsportal.com
http://www.sensorsportal.com/HTML/E-SHOP/PRODUCTS_4/Evaluation_board.htm